AJNR

Inner ear volumetric measurements using high-resolution 3D T2-weighted fast spin-echo MR imaging: initial experience in healthy subjects.

E R Melhem, H Shakir, S Bakthavachalam, C B MacDonald, J Gira, S D Caruthers and H Jara

AJNR Am J Neuroradiol 1998, 19 (10) 1819-1822
http://www.ajnr.org/content/19/10/1819

AJNR Am J Neuroradiol 19:1819–1822, November 1998

Inner Ear Volumetric Measurements Using High-Resolution 3D T2-Weighted Fast Spin-Echo MR Imaging: Initial Experience in Healthy Subjects

Elias R. Melhem, Huzeifa Shakir, Sivi Bakthavachalam, C. Bruce MacDonald, John Gira, Shelton D. Caruthers, and Hernan Jara

BACKGROUND AND PURPOSE: **Adult size is achieved in the inner ear labyrinth by approximately 25 weeks' gestation, and minimal variability in age, sex, side, and race is found after birth. In this study, we opted to determine the reproducibility of inner ear volumetric measurements generated from high-resolution heavily T2-weighted 3D fast spin-echo MR images.**

METHODS: **The temporal bones of 23 volunteers were imaged using a heavily T2-weighted 3D fast spin-echo MR imaging technique. The images were assessed by a neuroradiologist for the presence of inner ear configurational anomalies and, most important, for complete coverage of the inner ear labyrinth. Subsequently, the volume of the fluid in the inner ear was determined by two observers using a semiautomated segmentation algorithm. The mean, SD, range, and coefficient of variation of fluid volume in the inner ear were calculated. Age-, sex-, and side-related differences in the inner ear volumetric measurements were evaluated using analysis of variance. Interrater consistency in the inner ear volumetric measurements was evaluated by comparing the calculated coefficients of reliability.**

RESULTS: **Volumetric measurements were available from 46 inner ears in 23 volunteers. The mean volume was 227.8 mm^3 (SD, 24.4 mm^3), and the coefficient of variation was 10.7%. No age-, sex-, or side-related differences in the inner ear volumetric measurements were found (F ratios were 4.33, 5.04, and 0.26, respectively). Interrater consistency, as assessed by the coefficient of reliability, was 5.3%.**

CONCLUSION: **Reproducible volumetric measurements of the inner ear labyrinth can be obtained by applying a semiautomated segmentation algorithm to a heavily T2-weighted 3D fast spin-echo MR imaging data set. These volumetric measurements may help identify patients with congenital sensorineural hearing loss and normal inner ear configuration.**

Potentially disabling congenital sensorineural hearing loss is estimated to occur in one out of every 750 live births, with approximately 4800 hearing-impaired infants born yearly in the United States alone (1, 2). Early identification of significant hearing impairment and differentiation between nonprogressive (congenital) and progressive (delayed) hearing loss may minimize the loss of development of essential skills in speech, language, and social interactions (3, 4). Imaging has been helpful in identifying patients with gross labyrinthine configurational anomalies, thus placing them in the congenital group (5). However, only 15% of patients with congenital sensorineural hearing loss have gross configurational anomalies (5).

The goal of this study was to establish normative inner ear volumetric measurements that may allow identification of patients with congenital sensorineural hearing loss and no configurational anomalies. In addition, we attempted to determine the reproducibility of inner ear volumetric measurements generated from high-resolution heavily T2-weighted 3D fast spin-echo (FSE) MR images using a semiautomated segmentation algorithm. We hypothesized that no age-, sex- or side-related differences in inner ear volumetric measurements exist in healthy subjects.

Received May 12, 1998; accepted after revision August 3.

Supported in part by a research grant from Philips Medical Systems.

From the Departments of Radiology (E.R.M., H.J.) and Otolaryngology (C.B.M.), and the School of Medicine (H.S., S.B., J.G.), Boston University School of Medicine and Medical Center, and Philips Medical Systems (S.D.C.), Shelton, CT.

Address reprint requests to Elias R. Melhem, MD, Department of Radiology, Boston University Medical Center, 88 E Newton St, Atrium 2, Boston, MA 02118.

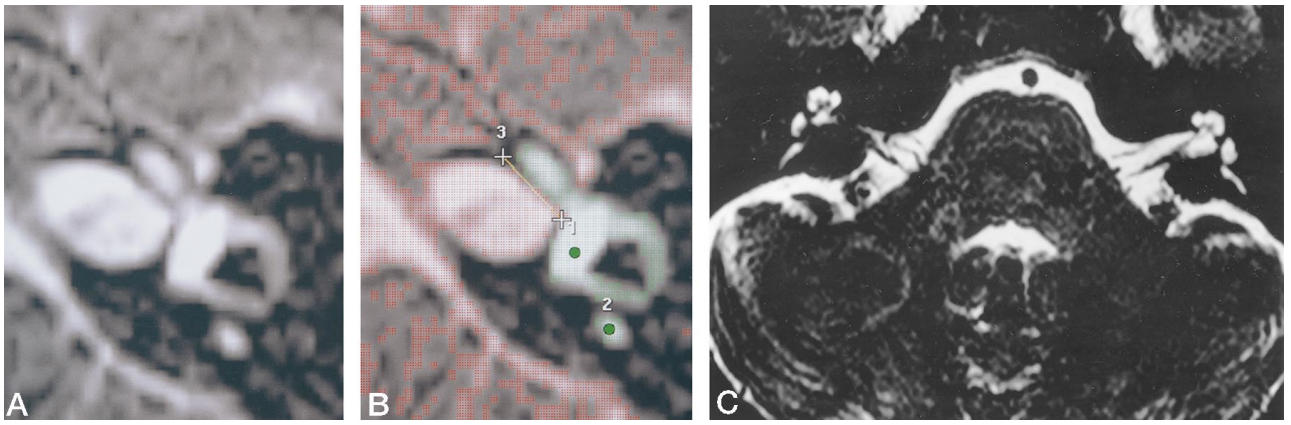

FIG 1. *A–C*, Axial T2-weighted FSE (2400/200) MR image obtained from the 3D data set at the level of the vestibule (*A*) and mid cochlea (*C*). On-line segmentation (*B*) resulted in highlighting in *red* all pixels with signal intensities above the set threshold. Pixels highlighted in *green* were those contiguous with the seed placed in the vestibule by the observers. Structures contiguous with but not part of the inner ear (ie, internal auditory canal) were manually excluded (*line 1–3*) from the selected volume of interest.

Methods

Temporal bone imaging was performed on a 1.5-T superconducting MR imaging system with maximum gradient capability of 10 $mT \cdot m^{-1}$ and slew rates of 10.0 $mT \cdot m^{-1} \cdot ms^{-1}$. MR images were obtained with a standard quadrature head coil operating in receive mode. General approval for evaluating new MR imaging techniques was obtained from the institutional review board before the study was initiated. Informed consent was obtained from all participating volunteers.

Twenty-three volunteers recruited over a 16-month period were imaged in the axial plane using the following MR imaging sequence: 3D Fourier transform FSE acquisition with imaging parameters of 2400/200/2 (TR/TE_{eff}/excitations), an echo train length of 18, and echo spacing of 16 milliseconds. Six overlapping sections were used, each divided into 0.6-mm-thick overcontiguous partitions. The sections were acquired in an interleaved fashion with a 50% overlap. The in-plane field of view was 16 cm with a 256 × 256 imaging matrix. Acquisition time was 5 minutes.

None of the 23 volunteers had a personal or family history of hearing loss and none had dysmorphic features, sustained CNS infections, or had been exposed to ototoxic medications. The volunteers consisted of 10 women and 13 men, ranging in age from 12 to 72 years (average age, 39 years).

The MR images from the 23 volunteers were assessed by an experienced neuroradiologist for the presence of inner ear configurational anomalies, endolymphatic duct/sac, degrading artifacts, and, most important, for complete coverage of the inner ear labyrinth (vestibule, semicircular canal, and cochlea). Forty-six inner ears were segmented independently by two trained observers from a total of 23 MR imaging data sets on an on-line workstation using commercially available software. Each data set was initially segmented in a gross fashion by simple thresholding. The threshold was set 3 SD below the mean measured from a region of interest placed in the fluid within the vestibule. Pixels below the threshold (ie, bone and brain parenchyma) were discarded, and pixels above the threshold (ie, CSF and fluid in the inner ear) were retained. Subpixel structures within the inner ear labyrinth, such as nerve rootlets, spiral laminae, and membranes, were not segmented out. In the retained pixels, a seed pixel was chosen within the vestibule. The volume of interest was grown iteratively from the original seed by including all pixels that were contiguous to the seed pixel or subsequently included pixels. Adjustments were made manually on each section to exclude pixels that were incorrectly included (ie, internal auditory canal) and to include pixels in the vestibule, semicircular canal, and cochlea that were missed by this automated selection criteria. Exclusion of unwanted pixels was conducted using a cropping tool, and inclusion of missed pixels was accomplished by dropping an extra seed pixel (Fig 1).

The mean, SD, range, and coefficient of variation of the fluid volumes in the inner ear were calculated to assess the reproducibility of our measurements. The mean, SD, and range of differences in volumes between left and right inner ears (L − R) were determined. Age-, sex-, and side-related differences in the inner ear volumetric measurements were evaluated using analysis of variance. Interrater consistency in ascertaining inner ear volumes was evaluated by comparing the calculated coefficients of reliability (2 × SD of the mean of the difference between two measurements divided by the mean of both measurements).

Inner Ear Volumetric Measurements from 3D T2-weighted Fast Spin-echo MR Imaging Data Sets

Volunteer	Age (y)/ Sex	Left Inner Ear Volume (mm^3)	Right Inner Ear Volume (mm^3)	L-R (mm^3)
1	12/M	258.3	252	6.3
2	19/F	198.3	235	−36.7
3	24/F	235	264.1	−29.1
4	26/F	240.5	234.6	5.9
5	27/M	257.1	184.7	72.4
6	28/M	256.6	272.1	−15.5
7	29/F	241.9	220.8	21.1
8	30/M	233	239.3	−6.3
9	33/F	216.3	243.5	−27.2
10	34/M	223.1	202.7	20.4
11	36/M	272.6	225	47.6
12	36/M	197.6	227.3	−29.7
13	39/M	237.7	257.8	−20.1
14	41/M	262.3	247.5	14.8
15	41/M	211.2	211.2	0
16	43/M	226.4	200.6	25.8
17	44/M	225.2	227.3	−2.1
18	48/M	258	233	25
19	48/F	172.3	195.5	−23.2
20	52/F	218	204.1	13.9
21	57/F	229.2	220.3	8.9
22	60/F	214	215.6	−1.6
23	72/F	197.6	183.3	14.3

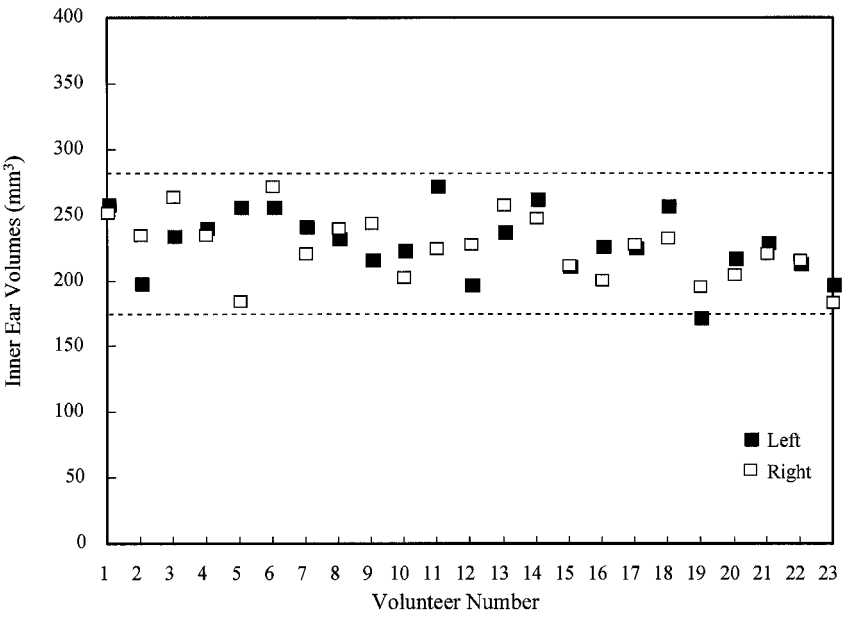

FIG 2. Scatter plot of the inner ear volumetric measurements with 95% confidence limits (±2 × SD) superimposed (*dashed lines*).

Results

Imaging of the inner ear was complete in all 23 volunteers, with no evidence of gross configurational anomalies or motion- or susceptibility-related artifacts. The endolymphatic duct and rugose portion of the endolymphatic sac were not identified in any of the imaged inner ears.

Volumetric measurements were available from 46 inner ears in 23 volunteers (see Table). The mean volume was 227.8 mm^3 (SD, 24.4 mm^3) and the coefficient of variation was 10.7%. The volumetric measurements ranged from 172.3 to 272.6 mm^3 (Fig 2). In the 23 volunteers, the mean difference between left and right inner ear volumes was −3.7 mm^3 (SD, 26.2 mm^3), ranging from −36.7 to 72.4 mm^3.

Using analysis of variance ($\alpha = 0.01$), no age-, sex-, or side-related differences in the inner ear volumes were found (F ratios were 4.33, 5.04, and 0.26, respectively). Interrater consistency, as assessed by the coefficient of reliability, was 5.3%.

Discussion

Findings of embryologic and anatomic studies have shown that adult configuration in the inner ear labyrinth is achieved by approximately 12 weeks' gestation, and adult size by approximately 25 weeks' gestation; minimal variability with age, sex, side, and race is found after birth (5–7). The implication is that patients with congenital sensorineural hearing loss may have a labyrinth with normal configuration but abnormal size, depending on the time of insult during gestation (6).

In this study, volumetric measurements of fluid in the inner ear labyrinth from data generated by high-resolution heavily T2-weighted FSE MR imaging showed little variability in the measured inner ear volumes with age, sex, and side. Unfortunately, we are unable to comment on the accuracy of the volumetric measurements because of the lack of direct anatomic correlation. However, our results do establish high reproducibility with a relatively narrow range, low coefficient of variation, and low interrater variability.

The intention was to provide a narrow and consistent range of normal inner ear volumetric measurements that may allow identification of patients with congenital sensorineural hearing loss who have sustained an insult between roughly 12 and 25 weeks' gestation (ie, small but grossly normal-appearing inner ear). In addition, the combination of inner ear high-resolution MR images and volumetric measurements may, in the future, allow stratification of patients with congenital sensorineural hearing loss into three major groups: those with gross inner ear configurational anomalies (insult before 12 weeks' gestation); those with volumetric abnormalities but no gross configurational anomalies (insult between 12 and 25 weeks' gestation); and those with no volumetric or configurational abnormalities (insult after 25 weeks' gestation). This stratification may have implications regarding the severity and progression of sensorineural hearing loss and may also help determine the time of fetal insult for medicolegal purposes.

FSE MR imaging techniques have been used by other investigators for imaging the inner ear labyrinth (8–10). These techniques offer several advantages, including efficient 3D imaging (8), reduced susceptibility-related artifacts at the petrous bone–inner ear fluid interface (perilymph and endolymph) (9, 10), lack of ionizing radiation, and heavy T2-weighting, which maximizes contrast between the inner ear fluid and adjacent bone. This contrast maximization has a definite beneficial effect on the ease of application and on the reproducibility of the implemented semiautomated segmentation algorithm.

The endolymphatic duct and rugose portion of the

endolymphatic sac were not included in the determination of volumetric measurements, owing to our inability to view these structures in any of our inner ear studies. Our inability to see the contents of the vestibular aqueduct probably resulted from diamagnetic susceptibility effects at the air-bone-fluid interface in the temporal bone. These effects were exaggerated by the relatively long echo spacing of our imaging technique. This finding represents a potential limitation regarding the reproducibility of our volumetric measurements as a function of the degree of aeration in the temporal bone. Future correlation with CT findings may help better define this effect. In addition, the relative paucity of free fluid in the vestibular aqueduct compared with other labyrinthine structures may be a reason for the inability of heavily T2-weighted imaging to show the contents of the vestibular aqueduct reliably (11–13).

Conclusion

Three-dimensional heavily T2-weighted FSE MR imaging techniques can be used for high spatial and contrast resolution imaging of the inner ear labyrinth. Reproducible volumetric measurements of the inner ear labyrinth can be obtained by applying a semiautomated segmentation algorithm to the MR imaging data set. These volumetric measurements may help identify patients with congenital sensorineural hearing loss and normal inner ear configuration.

References

1. Swigart ET, ed. ***Neonatal Hearing Screening***. San Diego: College Hill Press; 1986
2. Feinmesser M, Tell L. **Evaluation of methods on detecting hearing impairment in infancy and early childhood**. In: Mencher ET, ed. *Early Identification of Hearing Loss*. Basel: Karger; 1976:102–113
3. Davey PR. **Hearing loss in children of low birthweight.** *J Laryngol Otolaryngol* 1962;76:274–277
4. Dimitrius A, Petmezakes J, Papazesses G, et al. **Hearing loss in low birthweight infants.** *Am J Dis Child* 1982;136:602–604
5. Jackler RK, Luxford WM. **Congenital malformations of the inner ear: a classification based on embryogenesis.** *Laryngoscope* 1987; 97(Suppl 40):2–14
6. Pappas DG, Simpson LC, Randolph AM, et al. **High-resolution computed tomography: determination of the cause of pediatric sensorineural hearing loss.** *Laryngoscope* 1990;100:564–569
7. Nemzek WR, Brodie HA, Chong BW, et al. **Imaging findings of the developing temporal bone in fetal specimens.** *AJNR Am J Neuroradiol* 1996;17:1467–1477
8. Lee JN, King BD, Parker DL, et al. **High-resolution 3D imaging of the inner ear with modified fast spin-echo pulse sequence.** *J Magn Reson Imaging* 1996;1:223–225
9. Luedeke KM, Roeschmann P, Tischler R. **Susceptibility artifacts in NMR imaging.** *Magn Reson Imaging* 1985;3:329–343
10. Oehler M, Schmalbrock P, Chakeres DW. **Artifacts related to magnetic susceptibility differences between bone and air on high resolution MRI of the temporal bone.** *AJNR Am J Neuroradiol* 1995;16:1135–1143
11. Kodoma A, Sando I. **Dimensional anatomy of the vestibular aqueduct and endolymphatic sac (rugose portion) in human temporal bones: statistical analysis of 79 bones.** *Ann Otol Rhinol Laryngol Suppl* 1982;91:13–20
12. Schmalbrock P, Dailiana T, Chakeres DW, et al. **Submillimeter-resolution MR of the endolymphatic sac in healthy subjects and patients with Meniere disease.** *AJNR Am J Neuroradiol* 1996;17: 1707–1716
13. Harnsberger HR, Dahlen RT, Shelton C, et al. **Advanced techniques in magnetic resonance imaging in the evaluation of the large endolymphatic duct and sac.** *Laryngoscope* 1995;105:1037–1042

Please see the Editorial on page 1807 in this issue.